

Stellar Structure and the HR Diagram

PHYS 6260 Project Proposal

Brandon Pries

*School of Physics, Georgia Institute of Technology,
Atlanta, GA 30318*

March 8, 2023

1 Introduction

1.1 Overview

Stellar structure has been a topic of intense study for decades, as it lies at the intersection of several fields of physics: quantum mechanics, statistical mechanics, thermodynamics, hydrodynamics, transport processes, nuclear processes, particle physics, and electromagnetism, to name a few. To quote Dr. Dina Prialnik [1],

“This is, in fact, what distinguishes astrophysics from other physical disciplines. Astrophysics does not deal with a special, distinct class of effects and processes, as do the basic fields of physics. Nuclear physics, for example, deals exclusively with the atomic nucleus; there are many ramifications to this field of research, such as nuclear forces, nuclear structure and nuclear reactions, but they are all intimately connected. Nuclear physics has very little to do, say, with hydrodynamics, the study of the motion of continuous media. By contrast, astrophysics deals with complex phenomena, which involve processes of many different kinds. It has to lean, therefore, on all the branches of physics, and this makes for its special beauty. The theory of the structure and evolution of stars presents a unique opportunity to bring separate, seemingly unconnected physical theories under one roof.”

1.2 Literature Review

The history of our understanding of stellar structure is twofold: theoretical and observational. I will first consider the former.

One of the primary topics of early discussions of stellar structure was the source of the Sun’s energy. Initial theories included chemical burning, energy imparted from meteor showers, and gravitational contraction, but these sources predicted lifetimes that were wildly contradictory to geologic estimates for the age of Earth [2]. It was not until Bethe’s work in nuclear physics led him to postulate a thermonuclear source of energy for the sun (namely, the CNO cycle) [3].

The equations of state are usually derived from a combination of statistical mechanics, thermodynamics, and nuclear processes. Additional considerations are usually from fields like hydrodynamics and radiative transport. The equations of stellar structure come from assumptions like local thermodynamic equilibrium (LTE), continuity, energy transport/conservation of energy [1].

In modern times, these equations are solved numerically, and can also account for stellar evolution (i.e., explicit time dependence), including processes like chemical evolution, radial oscillations, mass loss, and stellar winds. Numerical suites like MESA [4] carry out these calculations for the equations of both stellar structure and stellar evolution.

On the observational side, observers in the early 20th century recorded spectra for many nearby stars to get a better understanding of stellar characteristics. Under Planck’s assumption that stars radiated like blackbodies [5], astronomers could estimate their surface temperatures. Then, by obtaining their distances from parallax measurements, astronomers could estimate their luminosities having measured the flux. Hertzsprung and Russell independently discovered a relationship between the luminosities and surface temperatures of stars [6–8], finding that many of them lie along a strip in the L - T phase space now called the main sequence; plots of stars in this phase space is now referred to as an HR diagram. Shortly thereafter, Annie Jump Cannon developed a classification scheme based on the strength of Balmer absorption lines and showed that this could be used as an analogy for the temperature axis [9, 10].

In recent years, much of this data-taking and cataloguing is done via telescopes, including Gaia [11, 12], a mission by the European Space Agency to take a census of $\mathcal{O}(10^9)$ stars in the Milky Way. This data has led to the most robust HR diagrams ever created [13].

→ GAIA'S HERTZSPRUNG-RUSSELL DIAGRAM

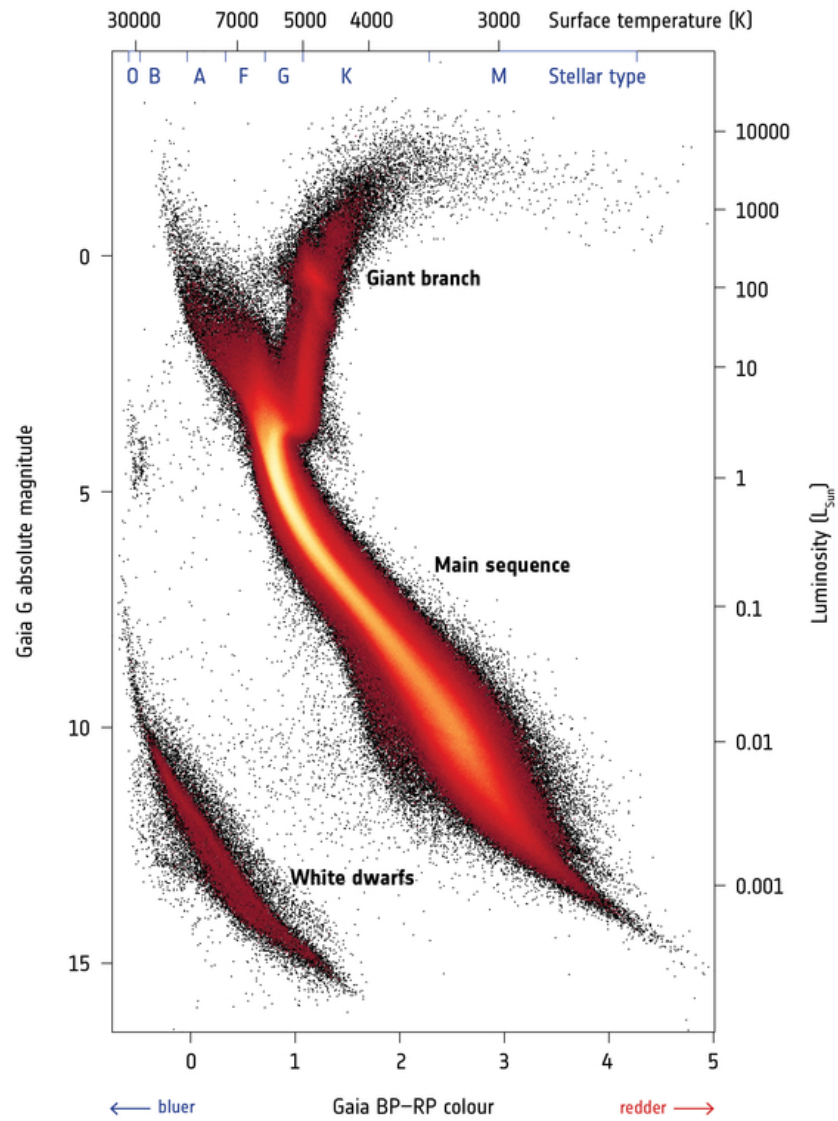


Figure 1: HR diagram of approximately 4.5 million stars from *Gaia* DR2 [13].

2 Simulations and Methodology

2.1 Scope and Goals

For this project, I will attempt to write code that can integrate the equations of stellar structure for a static star (neglecting time evolution). I will test my code by attempting to recreate the zero-age main sequence, parts of the giant branch, and the white dwarf sequence on the HR diagram. I can also explore the effects of metallicity on populations of stars in the HR diagram to see if they agree with observational results, and I can compare the profiles of different variables (e.g., P, L, T, ρ, X, Y, Z) for different types and masses.

Each star should be uniquely defined by its mass M and chemical composition $\vec{X} = [X, Y, Z]$; in principle, this composition will depend on the mass coordinate, but I will make the assumption that the composition is isotropic throughout the star. This is valid for the zero-age main sequence, and may be reasonable for white dwarfs, but is not a good approximation for giant stars that have concentric shells. I will need to develop a more sophisticated distribution of the chemical composition to properly model giant stars.

2.2 Equations of State and Stellar Structure

The equations of stellar structure (in concentric mass shells) are given by

$$\frac{\partial r(m)}{\partial m} = \frac{1}{4\pi r^2(m)\rho(m)} \quad (1a)$$

$$\frac{\partial P(m)}{\partial m} = -\frac{Gm}{4\pi r^4(m)} \quad (1b)$$

$$\frac{\partial L(m)}{\partial m} = \epsilon \quad (1c)$$

$$\frac{\partial T(m)}{\partial m} = \begin{cases} -\frac{3\kappa L(m)}{256\pi^2\sigma_{SB}r^4(m)T^3(m)} & \text{(radiative/conductive)} \\ \left(1 - \frac{1}{\gamma}\right) \frac{T(m)}{P(m)} \frac{\partial P(m)}{\partial m} & \text{(convective)} \end{cases} \quad ([14]) \quad (1d)$$

Note that (1d) is a piecewise equation that depends on the dominant energy transport mechanism.

The equations of state are given by

$$P = P_{\text{ions}} + P_e + P_{\text{rad}} \quad (2)$$

$$P_{\text{ions}} = \frac{\rho}{\mu_{\text{ions}} m_u} k_B T \quad (3a)$$

$$P_e = \begin{cases} \frac{\rho}{\mu_e m_u} k_B T & (\text{non-degenerate, non-relativistic}) \\ \frac{h^2}{20m_e} \left(\frac{3}{\pi}\right)^{2/3} \left(\frac{\rho}{\mu_e m_u}\right)^{5/3} & (\text{degenerate, non-relativistic}) \\ \frac{hc}{8} \left(\frac{3}{\pi}\right)^{1/3} \left(\frac{\rho}{\mu_e m_u}\right)^{4/3} & (\text{degenerate, relativistic}) \end{cases} \quad (3b)$$

$$P_{\text{rad}} = \frac{4}{3} \frac{\sigma_{SB}}{c} T^4 \quad (3c)$$

These equations give us the relationship between P , T , and ρ . Since P and T are tracked variables, we can solve these equations for ρ ; however, these are non-linear equations when matter is degenerate, so we may need to use root-finding to calculate ρ .

For the luminosity gradient in (1c), the energy generation is [15]

$$\epsilon \approx \begin{cases} 2.4 \cdot 10^3 \frac{\rho X^2}{T^{2/3}} \exp\left(-\frac{3.380 \cdot 10^3}{T^{1/3}}\right) & (pp\text{-chains}) \\ 4.4 \cdot 10^{24} \frac{\rho X Z_{\text{CNO}}}{T^{2/3}} \exp\left(-\frac{15.288 \cdot 10^3}{T^{1/3}}\right) & (\text{CNO cycle}) \\ 5.1 \cdot 10^{28} \frac{\rho^2 Y^3}{T^3} \exp\left(-\frac{4.4027 \cdot 10^9}{T}\right) & (\text{triple-}\alpha) \end{cases} \quad (4)$$

For the temperature gradient in (1d), we need κ , which accounts for both radiative and conductive opacity. These come from multiple sources (namely, electron scattering, free-free absorption, bound-free absorption, electron conduction, and photon conduction) [15, 16]:

$$\frac{1}{\kappa} = \frac{1}{\kappa_{\text{rad}}} + \frac{1}{\kappa_{\text{cond}}} \quad (5)$$

$$\kappa_{\text{rad}} = \kappa_{e,\text{rad}} + \kappa_{\text{f-f}} + \kappa_{\text{b-f}} \quad (6a)$$

$$\kappa_{\text{cond}} = \kappa_{e,\text{cond}} + \kappa_{\gamma} \quad (6b)$$

$$\kappa_{e,\text{rad}} = 0.02(1 + X) \quad (7a)$$

$$\kappa_{\text{f-f}} \sim 10^{22} \frac{Z^2}{\mu_{\text{ions}} \mu_e} \rho T^{-7/2} \quad (7b)$$

$$\kappa_{\text{b-f}} \sim 10^{24} Z(1 + X) \rho T^{-7/2} \quad (7c)$$

$$\kappa_{e,\text{cond}} = \frac{32\pi\sigma_{SB}T^3}{3k_B\rho} \left(\frac{m_e}{3k_BT}\right)^{1/2} \left(\frac{\bar{Z}e^2}{4\pi\epsilon_0 k_BT}\right)^2 \quad (8a)$$

$$\kappa_{\gamma} = \sqrt{3}\bar{Z} \frac{P_{\text{rad}}}{P_e} \left(\frac{m_e c^2}{k_BT}\right)^{5/2} \kappa_{e,\text{cond}} \quad (8b)$$

These equations are supplemented by the definitions of the mean molecular weights [1]:

$$\frac{1}{\mu_{\text{ions}}} = \sum_i \frac{X_i}{\mathcal{A}_i} \quad (9a)$$

$$\frac{1}{\mu_e} = \sum_i \frac{X_i Z_i}{\mathcal{A}_i} \quad (9b)$$

2.3 Boundary Conditions

Our numerical simulations require boundary conditions at the center and the surface. At the center, we can take

- $\lim_{m \rightarrow 0} m = 0$
- $\lim_{m \rightarrow 0} r(m) = 0$
- $\lim_{m \rightarrow 0} L(m) = 0$
- $\lim_{m \rightarrow M_0} \rho(m) = \rho_c = 5.9905 \frac{3}{4\pi} \left(\frac{M}{M_\odot} \right) \left(\frac{R}{R_\odot} \right)^{-3} \quad ([17])$
- $\lim_{m \rightarrow M_0} P(m) = P_c = 0.7701 G \left(\frac{M}{M_\odot} \right)^2 \left(\frac{R}{R_\odot} \right)^{-4} \quad ([17])$
- $\lim_{m \rightarrow M_0} T(m) = T_c = \frac{m_u}{k_B \left(\frac{1}{\mu_{\text{ions}}} + \frac{1}{\mu_e} \right)} \frac{P_c}{\rho_c} \approx 0.5385 \frac{G m_u}{k_B \left(\frac{1}{\mu_{\text{ions}}} + \frac{1}{\mu_e} \right)} \left(\frac{M}{M_\odot} \right) \left(\frac{R}{R_\odot} \right)^{-1} \quad (3)$

where the last equation (T_c) neglects radiation pressure at the center. Here, m, r, L are set initial conditions, and P_c, T_c are guesses. At the surface, we have

- $\lim_{m \rightarrow M} m = M$
- $\lim_{m \rightarrow M} L(m) = L_s \approx \left(\frac{M}{M_\odot} \right)^{3.5} L_\odot \quad ([18])$
- $\lim_{m \rightarrow M} r(m) = R = \begin{cases} \left(\frac{M}{M_\odot} \right)^{0.8} R_\odot & M \leq M_\odot \\ \left(\frac{M}{M_\odot} \right)^{0.57} R_\odot & M > M_\odot \end{cases} \quad ([19])$
- $\lim_{m \rightarrow M} T(m) = T_s = \left(\frac{L_s}{4\pi R^2 \sigma_{SB}} \right)^{1/4}$

- $\lim_{m \rightarrow M} P(m) = P_s = \frac{2}{3} \frac{GM}{\kappa_s R^2} + \frac{2}{3c} \frac{L_s}{4\pi R^2}$ ([19])

Here, M, P_s, T_s are set initial conditions, and R, L_s are guesses.

If we set the optical depth $\tau = \frac{2}{3}$ at the photosphere, then by neglecting the conductive opacity and the opacity due to electron scattering, we can approximate the surface density as [19]

$$\rho(M) = \rho_s = \sqrt{\frac{2}{3}} \left(10^{22} \frac{Z^2}{\mu_{\text{ions}} \mu_e} T^{-7/2} + 10^{24} Z(1+X) T^{-7/2} \right)^{-1/2} \quad (10)$$

This gives us

$$\kappa_s = \kappa_{\text{f-f}}(\rho_s, T_s) + \kappa_{\text{b-f}}(\rho_s, T_s) \quad (11)$$

2.4 Perturbations and Shooting

We will use the definition $\vec{z} = [r, P, L, T]$ (and \vec{z}_0 for the corresponding initial conditions) to summarize the variables we must keep track of. The primary simulation will be simultaneous inward and outward integration using the equations of stellar structure subject to the boundary conditions specified in 2.3. Our solutions \vec{z}_1 and \vec{z}_2 will meet in the middle at some mass m_{mid} ; however, it is unlikely that they will agree. Therefore, we must use a shooting algorithm to determine how to proceed.

If we define $\mathcal{R} = \vec{z}_2(m_{\text{mid}}) - \vec{z}_1(m_{\text{mid}})$, we can use this to determine how to perturb our initial conditions to achieve a more accurate solution. If we let \vec{x} be our vector of guessed boundary conditions (i.e., $\vec{x} = [R, P_c, L_s, T_c]$), then we want to solve the equations

$$\sum_j \frac{\partial \mathcal{R}_i}{\partial x_j} \delta x_j = -\mathcal{R}_i \quad (12)$$

for the perturbations δx_j . Note that each partial derivative $\frac{\partial}{\partial x_j}$ will itself require another inward/outward integration with some estimated perturbation to x_j , though this integration can calculate the derivative for all \mathcal{R}_i 's.

2.5 Data

To check the results of my models, I plan to compare them to publicly-available data from the Gaia mission [12]; specifically, I will plot my results on the HR diagram against a backdrop of Gaia data (see Fig. 1).

References

- [1] D. Prialnik. *An Introduction to the Theory of Stellar Structure and Evolution*. 2nd ed. Cambridge University Press, 2010. ISBN: 978-0-521-86604-0.
- [2] H. Kragh. “The Source of Solar Energy, ca. 1840-1910: From Meteoric Hypothesis to Radioactive Speculations”. In: *EPJ H* 41.4-5 (Sept. 9, 2016). DOI: [10.1140/epjh/e2016-70045-7](https://doi.org/10.1140/epjh/e2016-70045-7). URL: <https://arxiv.org/abs/1609.02834>.
- [3] H. A. Bethe. “Energy Production in Stars”. In: *Phys. Rev.* 55 (5 Mar. 1939), pp. 434–456. DOI: [10.1103/PhysRev.55.434](https://doi.org/10.1103/PhysRev.55.434). URL: <https://link.aps.org/doi/10.1103/PhysRev.55.434>.
- [4] B. Paxton et al. “Modules for Experiments in Stellar Astrophysics (MESA)”. In: *The Astrophysical Journal Supplement Series* 192.1 (Dec. 2010), p. 3. DOI: [10.1088/0067-0049/192/1/3](https://doi.org/10.1088/0067-0049/192/1/3). URL: <https://arxiv.org/abs/1009.1622>.
- [5] Wikipedia. *Planck’s law*. Mar. 2023. URL: https://en.wikipedia.org/wiki/Planck%27s_law.
- [6] E. Hertzsprung. “Über die Sterne der Unterabteilungen *c* und *ac* nach der Spektralklassifikation von Antonia C. Maury”. In: *Astronomische Nachrichten* 179.24 (Jan. 1909), p. 373. DOI: [10.1002/asna.19081792402](https://doi.org/10.1002/asna.19081792402).
- [7] H. Rosenberg. “Über den Zusammenhang von Helligkeit und Spektraltypus in den Plejaden”. In: *Astronomische Nachrichten* 186.5 (Oct. 1910), p. 71. DOI: [10.1002/asna.19101860503](https://doi.org/10.1002/asna.19101860503).
- [8] H. Russell. “Relations Between the Spectra and Other Characteristics of the Stars”. In: *Popular Astronomy* 22 (May 1914), pp. 275–294.
- [9] A. J. Cannon and E. C. Pickering. “The Henry Draper catalogue 0h, 1h, 2h, and 3h”. In: *Annals of Harvard College Observatory* 91 (Jan. 1918), pp. 1–290.
- [10] Wikipedia. *Annie Jump Cannon*. Jan. 2023. URL: https://en.wikipedia.org/wiki/Annie_Jump_Cannon.
- [11] European Space Agency. *Gaia homepage*. URL: <https://www.cosmos.esa.int/web/gaia>.
- [12] F. van Leeuwen et al (Gaia Collaboration). *Gaia DR3 documentation*. Gaia DR3 documentation, European Space Agency; Gaia Data Processing and Analysis Consortium. Online at <https://gea.esac.esa.int/archive/documentation/GDR3/index.html>. June 2022.

- [13] C. Babusiaux et al (*Gaia* Collaboration). “*Gaia* Data Release 2: Observational Hertzsprung-Russel Diagrams”. In: *A&A* 616 (Aug. 2018), A10. DOI: [10 . 1051 / 0004 – 6361 / 201832843](https://doi.org/10.1051/0004-6361/201832843). URL: <https://arxiv.org/abs/1804.09378>.
- [14] Wikipedia. *Stellar structure*. Jan. 2023. URL: https://en.wikipedia.org/wiki/Stellar_structure.
- [15] C. Hansen, S. Kawaler, and V. Trimble. *Stellar Interiors: Physical Principles, Structure, and Evolution*. 2nd ed. Springer, 2004. ISBN: 978-1-4612-6497-2. DOI: [10.1007/978-1-4419-9110-2](https://doi.org/10.1007/978-1-4419-9110-2).
- [16] K. Wood. Lecture slides for AS 3003 at the University of St. Andrews. URL: <http://www-star.st-and.ac.uk/~kw25/teaching/stars/STRUC7.pdf>.
- [17] E. Brown. GitHub code for stellar integration for AST 304 at Michigan State University. Dec. 2020. URL: <https://github.com/MSU-AST304-FS2020/Project3-main-sequence>.
- [18] Wikipedia. *Mass-luminosity relation*. Apr. 2022. URL: https://en.wikipedia.org/wiki/Mass%E2%80%93luminosity_relation.
- [19] R. Ciardullo. Lecture notes for A534 at Penn State University. URL: <http://personal.psu.edu/rbc3/A534/>.